

Interaction of fullereneol with lysozyme investigated by experimental and computational approaches

This article has been downloaded from IOPscience. Please scroll down to see the full text article.

2008 Nanotechnology 19 395101

(<http://iopscience.iop.org/0957-4484/19/39/395101>)

View [the table of contents for this issue](#), or go to the [journal homepage](#) for more

Download details:

IP Address: 130.91.198.166

The article was downloaded on 25/06/2013 at 17:48

Please note that [terms and conditions apply](#).

Interaction of fullereneol with lysozyme investigated by experimental and computational approaches

Sheng-Tao Yang¹, Haifang Wang^{1,3}, Lin Guo¹, Yang Gao¹,
Yuanfang Liu^{1,2} and Aoneng Cao^{2,3}

¹ Beijing National Laboratory for Molecular Sciences; Department of Chemical Biology, College of Chemistry and Molecular Engineering, Peking University, Beijing 100871, People's Republic of China

² Institute of Nanochemistry and Nanobiology, Shanghai University, Shanghai 200444, People's Republic of China

E-mail: haifangw@pku.edu.cn and ancao@shu.edu.cn

Received 17 April 2008, in final form 17 July 2008

Published 8 August 2008

Online at stacks.iop.org/Nano/19/395101

Abstract

The potential biomedical applications of fullereneol $C_{60}(OH)_x$ ($x \approx 24$) have been extensively studied. However, the structural information of the interaction of fullereneol with the bio-system at the molecular level, which is essential for understanding its bioactivity and toxicity, is still missing. In this study, lysozyme was selected as a model protein to investigate the interaction between fullereneol and biomolecules. A strong induced circular dichroism (CD) signal of achiral fullereneol was observed after binding with lysozyme. Activity assay shows that lysozyme activity is inhibited significantly by fullereneol. No heat capacity difference between the folded and unfolded states of lysozyme was measured by differential scanning calorimetry (DSC) in the presence of fullereneol, indicating that fullereneol prefers to bind with the hydrophobic residues. Both experimental and Autodock computational results suggest that the binding site on lysozyme for fullereneol is close to Trp 62, and a π - π stacking interaction might play an important role in binding.

 Supplementary data are available from stacks.iop.org/Nano/19/395101

1. Introduction

Since the discovery, fullerene, metallofullerene and their derivatives have raised great interest for their potential biomedical applications among scientists [1]. Notably, the water-soluble hydroxylated fullerene, fullereneol, has been applied in many biomedical areas. Fullereneol can inhibit tumor cell growth via blocking the microtubule assembly *in vitro* [2] and metallofullereneol $Gd@C_{82}(OH)_{22}$ shows strong antitumor activity in tumor-bearing mice without side effects [3]. Because of the impressive antioxidative potential and radical scavenging activity, fullereneol also has been used to reduce the cardiotoxicity [4] and provide radioprotection [5]. Recent studies indicate that fullereneol inhibits the M-MuLV reverse transcriptase activity *in vitro*, manifesting its potential

in treatment of diseases induced by RNA viruses [6]. It is also reported that fullereneol can inhibit the allergic response [7].

To achieve a better understanding of the bioactivity and toxicity of fullereneol, the study of the interaction of fullereneol with the bio-system at a molecular level is essential, but is still scarce at present. Since proteins carry out most of the functions in the bio-system, it is important to study the interactions between fullereneol and proteins. Previous studies have revealed that the adsorption of protein onto different nanoparticles would cause obviously loss of activity and changes of conformation [8]. It is also reported that proteins could be adsorbed on pristine fullerene [9–12] or its derivatives, such as tris-malonic acid fullerene and organophosphate-containing fullerene [13–15]. Proteins adsorbed on nanoparticles may lose their catalytic activity or activate the coagulation and immune response [16]. This basic information about fullereneol and proteins would

³ Authors to whom any correspondence should be addressed.

help to explain the pharmacological activity of fullereneol and indicate its potential toxicity.

Lysozyme from hen egg white is one of the best characterized and the most extensively studied proteins. As a widely existing enzyme, lysozyme can hydrolyze the glycosidic bond, leading to the solubilization of bacterial cell walls. Lysozyme's biological functions [17–19] include antimicrobial, antitumor and immunomodulatory activities, etc. Lysozyme's structure [20], folding/unfolding [21, 22], amyloid aggregation [23] and many other properties [24, 25] have been studied in detail. Lysozyme has also been widely used as a model protein in non-biological fields such as nanoscience [26]. And, unlike some other model proteins such as albumin, the change of lysozyme activity can be taken as a measure to study the function change of a protein.

In this study, the influences of fullereneol on the function and conformation of lysozyme were studied by various experimental techniques, including circular dichroism (CD), fluorescence spectroscopy and differential scanning calorimetry (DSC). The binding of fullereneol with lysozyme was also studied computationally using the most cited docking program, Autodock (autodock.scripps.edu). Both the experimental and computational results generated a compatible binding model for fullereneol and lysozyme interaction.

2. Experimental details

2.1. Materials

Lysozyme from hen egg white and *M. lysodeikticus* were purchased from Sigma Co (St Louis, USA). Lysozyme had been dialyzed against distilled water for two days and then lyophilized before use. Other chemicals used were of analytical grade.

2.2. Preparation of fullereneol

Fullereneol $C_{60}(OH)_x$ ($x \approx 24$) was prepared and characterized following the method previously described [27, 28]. Briefly, 80 mg of C_{60} was solubilized in 60 ml of benzene. Then, 10 ml of KOH aqueous solution (1.0 g ml^{-1}) and 0.2 ml of tetra-*n*-butylammonium hydroxide were added to the solution and stirred for several minutes. After the color of the solution faded, the benzene was removed by vacuum distillation. The mixture was stirred for another 60 h. With the addition of 20 ml water, the mixture was stirred for 12 h and diluted with water. After filtration, the solubilized fullereneols were precipitated by methanol. The precipitate was solubilized with water and a Sephadex G-25 ($\Phi 16 \times 250 \text{ mm}$) column was employed for purification. The product was characterized by transmission electron microscope (TEM, JEM-200CX, Japan), laser light scattering spectroscopy (DLS, ALV/DLS/SLS-5022F, Germany), UV-vis spectrum (PE lambda 35 UV/vis, Perkin Elmer, USA), fluorescence spectrum (FL, F4500 fluorescence spectrometer, Hitachi, Japan), infrared spectroscopy (IR, Magna-IR 750, Nicolet, USA), nuclear magnetic resonance (NMR, ARX400, Bruker, Switzerland), elementary analysis (vario EL, Elementar Analysensysteme GmbH, Germany) and x-ray photoelectron spectroscopy (XPS, Kratos, UK).

2.3. Lysozyme activity assay

A lysozyme solution with a concentration of $3.5 \mu\text{M}$ was prepared by dissolving purified lysozyme in 40 mM phosphate buffer (pH 6.2). After incubating with different dosages of fullereneol for 8 h at room temperature, the enzyme activity of free lysozyme and mixtures was determined as described by Shugar [29]. Briefly, 1.5 ml of *M. lysodeikticus* (0.25 mg ml^{-1}) was added to the 1 cm quartz cuvette and the absorbance was recorded at 450 nm. An aliquot of fullereneol/lysozyme mixture ($100 \mu\text{l}$) was added to the cuvette and the dynamic absorbance was recorded. The initial slope (k) of the dynamic absorbance curve (the curve of the absorbance at 450 nm versus time) was calculated. The relative activity is expressed as $k_{\text{mix}}/k_{\text{free}} \times 100\%$, where k_{mix} is the initial slope of the dynamic absorbance curve of the mixture and k_{free} is the initial slope of the dynamic absorbance curve of free lysozyme.

2.4. DSC measurement

Thermal denaturation was performed on Micro-DSC III (Setaram, France). A mixture of $280 \mu\text{M}$ lysozyme and $430 \mu\text{M}$ fullereneol in 40 mM phosphate buffer (pH 6.2) was incubated for 8 h before measurement. The DSC measurements were carried out at a scan rate of 1°C per min using $430 \mu\text{M}$ fullereneol in phosphate buffer (pH 6.2) solution as the blank. The DSC of the free lysozyme was also performed in the same manner.

2.5. CD spectroscopy

The CD spectra were recorded on JY CD6 (JobinYvon, France). Lysozyme was incubated with fullereneol for 8 h. The far-ultraviolet CD (far-UV CD) measurements were performed in a 1 mm quartz cuvette with a protein concentration of $18 \mu\text{M}$ in 40 mM phosphate buffer (pH 6.2). The sample was scanned from 250 to 200 nm. The near-ultraviolet CD (near-UV CD) measurements were performed in a 1 cm quartz cuvette with a protein concentration of $70 \mu\text{M}$. The sample was scanned over a wavelength range from 310 to 260 nm. For both measurements, a fullereneol solution with the same concentration was used as the blank sample. Each spectrum presents an average of four scans.

2.6. Fluorescence spectroscopy and association constant determination

Fluorescence spectra excited at 280 or 295 nm were recorded between 310 and 470 nm on a F4500 fluorescence spectrometer, with 5 nm slit for both excitation and emission. Lysozyme ($2 \mu\text{M}$) in 40 mM phosphate buffer (pH 6.2) was incubated in the absence or presence of fullereneol for 8 h before recording spectra, and the concentration of fullereneol changed from $0.2 \mu\text{M}$ till no apparent fluorescence change. Experiments were repeated four times.

The association constant (K_a) was estimated based on a simple 1:1 binding model:



$$K_a = [PL]/[P] \cdot [L] \quad (2)$$

where K_a is the association constant, $[P]$ is the equilibrium concentration of free lysozyme, $[L]$ is the equilibrium concentration of free fullerene and $[PL]$ is the equilibrium concentration of the complex PL. $[PL]$ was calculated from the normalized fluorescence change. $[P]$ equals $[P]_{\text{tot}} - [PL]$, where $[P]_{\text{tot}}$ represents the total concentration of lysozyme, which is $2 \mu\text{M}$ in the experiment. $[L]$ equals $[L]_{\text{tot}} - [PL]$, where $[L]_{\text{tot}}$ represents the total concentration of fullerene in solution, which was known. Let ν represent the ratio of lysozyme bound with fullerene, which equals the normalized fluorescence change ΔF :

$$\Delta F = \nu = [PL]/[P]_{\text{tot}}. \quad (3)$$

$$\text{Since } [P]_{\text{tot}} = [P] + [PL]. \quad (4)$$

From the above equations, we have

$$1/\Delta F = 1/\nu = 1 + 1/K_a \cdot [L]. \quad (5)$$

Therefore, $1/\Delta F$ was plotted versus $1/[L]$ using Origin 7.5 (OriginLab, USA) to obtain K_a [30].

2.7. Autodocking

Autodock is the most cited program to dock small molecule ligands to proteins, and it has also been used to study the interactions between protein and fullerene derivatives [31, 32]. Therefore, Autodock is used in our study to simulate the detailed binding model between lysozyme and fullerene.

The structure of $\text{C}_{60}(\text{OH})_{24}$ was built by CS Chem3D Ultra (CambridgeSoft). The structure used for hen egg white lysozyme came from the PDB code: 1HEL. Docking was performed using Autodock 4.0 (autodock.scripps.edu). $\text{C}_{60}(\text{OH})_{24}$ and lysozyme molecules were first prepared by AutoDockTools 1.4.6 (autodock.scripps.edu) [33], including adding polar hydrogen atoms and assigning Kollman united atom charges to lysozyme, computing Gasteiger charges for $\text{C}_{60}(\text{OH})_{24}$, setting 24 rotatable bonds for $\text{C}_{60}(\text{OH})_{24}$ and setting flexible residue for lysozyme. Firstly, a 'blind docking' was carried out with a large grid volume ($80 \times 80 \times 80$ with 0.503 \AA grid spacing) covering the entire surface of lysozyme to find the preferred binding regions on the lysozyme surface for fullerene. In the blind docking, lysozyme was set as rigid and all the 24 C–O bonds of $\text{C}_{60}(\text{OH})_{24}$ were set as rotatable. Thirty binding models were generated. Each was picked from an individual run as the lowest energy conformation among a maximum of 2 500 000 evaluations. Then, the second round of dockings with a small fine grid of 0.253 \AA grid spacing was carried out to evaluate each possible binding site found in the first round 'blind docking'. Finally, a flexible docking was carried out to find out the best binding model for fullerene–lysozyme and to calculate the binding energy and the association constant as well.

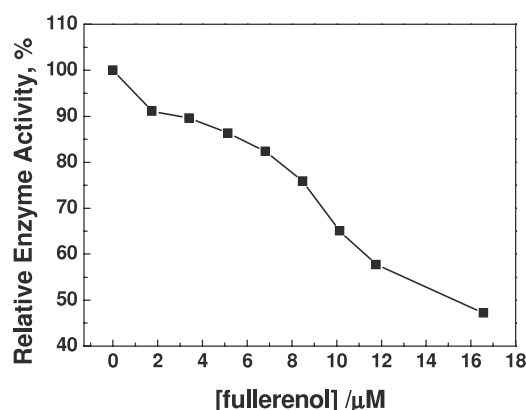


Figure 1. Relative enzyme activity of lysozyme after being incubated with different concentrations of fullerene.

3. Results and discussion

The detailed characterizations of fullerene $\text{C}_{60}(\text{OH})_x$ ($x \approx 24$) can be found in supporting information (available at stacks.iop.org/Nano/19/395101). The value of x is not identical for each synthesized fullerene. According to the XPS results the atom ratio of carbon to oxygen is 5:2, indicating that on average 24 hydroxyl groups attach to one fullerene cage (see supporting information available at stacks.iop.org/Nano/19/395101). The XPS results are taken to determine the number of hydroxyl groups, because the elementary analysis is not precise in characterizing of hydroxylated fullerene [3, 27, 34]. Therefore, in the text, $\text{C}_{60}(\text{OH})_x$ ($x \approx 24$) is taken in all experimental content, while an exact 24 hydroxyl groups are settled on in the computational study.

3.1. Activity assay

The activity of lysozyme was evaluated by its ability to dissolve the bacterial cell wall of *M. lysodeikticus*. Figure 1 shows that, while the fullerene concentration increases, the activity of lysozyme decreases significantly. When the molar ratio of fullerene/lysozyme is 1:1 ($3.4 \mu\text{M}$ of fullerene), nearly 90% of enzyme activity remains. But when the molar ratio reaches 5:1 ($16.6 \mu\text{M}$ of fullerene), lysozyme loses half of its activity. Clearly, fullerene has a great influence on the activity of lysozyme. This also implies that the adsorption of fullerene might induce conformational changes of lysozyme.

The loss of enzyme activity might lead to a series of pharmacological and toxicological consequences. For the pharmacological applications, the reported inhibition of the M-MuLV reverse transcriptase activity manifests the potential of fullerene in treatment of diseases induced by RNA viruses [6]. Also, other fullerene derivatives have been reported to inhibit the HIV enzyme activity [35–37]. The antiproliferative effect of fullerene is observed and attributed to the inhibition of the growth-related signal, protein tyrosine kinase [38]. For the toxicological profiles, many *in vitro* and *in vivo* studies have proved that fullerene shows low or no toxicity at low concentration [39–42].

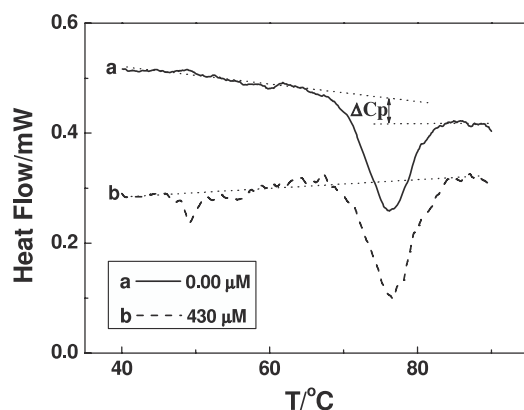


Figure 2. DSC spectra of the free lysozyme and the fullerene-lysozyme complex.

3.2. DSC measurements

The thermal denaturation temperature (T_d) of the free lysozyme is 76.2°C, while in the presence of fullerene, T_d increases to 76.6°C (figure 2). The enthalpy of thermal denaturation obtained from DSC measurements is 460.4 kJ mol⁻¹ for free lysozyme and 576.3 kJ mol⁻¹ for the mixture. These demonstrate that fullerene improves the thermal stability of lysozyme slightly.

An interesting feature is that, in the presence of fullerene, the folded and unfolded states of lysozyme have almost the same heat capacity. The DSC data of the free lysozyme show a typical feature of a protein thermal unfolding process, i.e. the heat capacity of the unfolded state is much greater than that of the folded state, mainly due to the temperature-dependent ordering of water molecules around hydrophobic residues which are solvent-accessible in the unfolded state [43]. However, in the presence of fullerene, there is no heat capacity difference between the folded and unfolded states of lysozyme. This indicates that those hydrophobic residues exposed after unfolding are not water-accessible in the presence of fullerene. In other words, fullerene readily binds with those exposed hydrophobic residues.

3.3. CD measurements

CD spectroscopy is a widely used technique for the study of solution structures of proteins, with far-UV CD spectra showing the information of a protein's secondary structure and near-UV CD spectra for a protein's tertiary structure. Figure 3(a) shows the far-UV CD spectra of lysozyme. When the fullerene concentration increases, the ellipticity ($[\theta]$) at 208 and 220 nm decreases, which means the decrease of helical structure. The percentage of α -helix in lysozyme was estimated by using $[\theta]$ at 208 nm [44]. When the molar ratio of fullerene/lysozyme reaches 1:1, the α -helix content decreases to about 29.1% (about 41.8% for the free lysozyme). Although the secondary structure has been partially disordered, the enzyme activity remains at this molar ratio.

The near-UV CD spectra of lysozyme incubated with fullerene show significant and interesting changes (figure 3(b)). For proteins, the near-UV CD change indicates

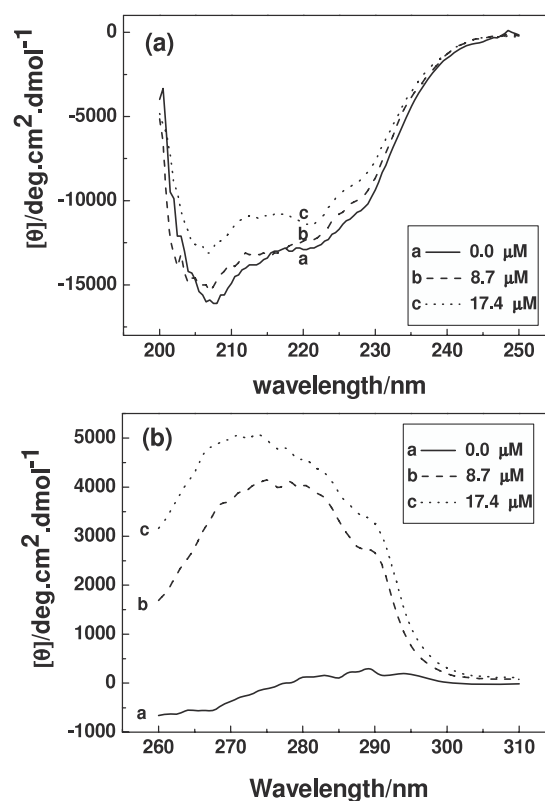


Figure 3. (a) Far-UV CD spectra of lysozyme incubated with different concentrations of fullerene. (b) Near-UV CD spectra of lysozyme incubated with different concentrations of fullerene.

an environment (or tertiary structure) change of the aromatic residues, such as phenylalanine (Phe), tyrosine (Tyr) and tryptophan (Trp). Fullerene has no near-UV CD signals (data not shown), because the hydroxyl groups are distributed randomly on the carbon cage. However, the ellipticity value of the lysozyme-fullerene complex is more than one order of magnitude greater than that of the free lysozyme alone. At a wavelength between 266.0 and 277.5 nm, the ellipticities of lysozyme are negative, while the ellipticities of the lysozyme-fullerene complex are significantly positive. These results indicate that the dramatic change of the near-UV CD signal should be mainly the induced CD of fullerene, i.e. the specific binding with lysozyme broke the symmetry of fullerene. Interaction with fullerene will also change the near-UV CD of lysozyme, but it should be minor, because the lysozyme's near-UV CD signal is at least one magnitude less than this huge increase. To our knowledge, this is the first report of the noncovalent-binding-induced near-UV CD from the achiral fullerene.

3.4. Fluorescence spectra study

Intrinsic fluorescence of protein mainly comes from Trp and Tyr residues. Both Trp and Tyr can be excited at 280 nm; however, only Trp can be excited at 295 nm. Due to the higher absorbance coefficient and higher fluorescence quantum yield, Trp is about fivefold more sensitive than Tyr. The intrinsic fluorescence intensity of lysozyme decreases

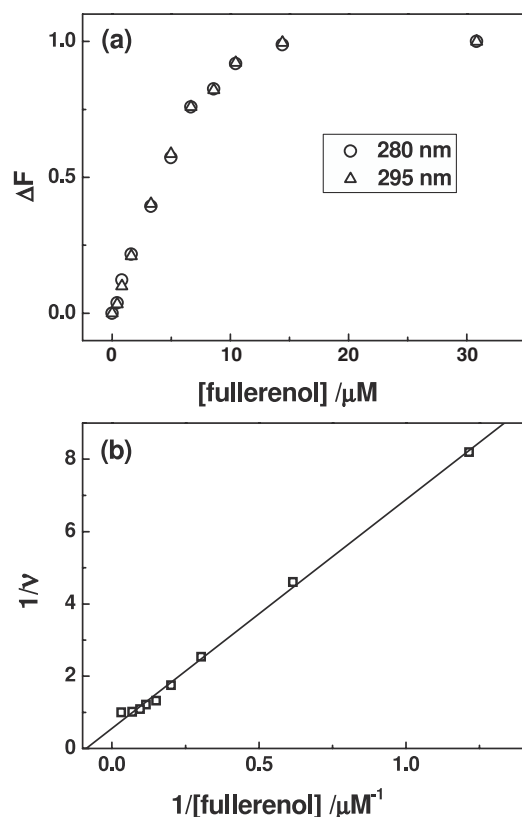


Figure 4. Intrinsic fluorescence change of lysozyme incubated with different concentrations of fullereneol. (a) Normalized fluorescence changes at 340 nm versus the concentration of free fullereneol: open circle, excited at 280 nm; open triangle, excited at 295 nm; (b) double-reciprocal plot of the change of fluorescence intensity (ΔF) at 340 nm versus the concentration of free fullereneol.

moderately with increasing fullereneol concentration. To compare the fluorescence changes between the spectra excited at 280 and 295 nm, they had to be normalized. Figure 4(a) shows the normalized fluorescence changes at 340 nm. It can be seen that the normalized fluorescence changes are almost the same for the 280 and 295 nm excited spectra, suggesting that the change may mainly come from Trp residues, whether by direct interaction with fullereneol or indirect conformational change caused by the interaction between lysozyme and fullereneol. Since Trp 62 and Trp 63 are located near to the active site, given the fact that the activity of lysozyme decreases with the binding of fullereneol, the binding site for fullereneol is very likely close to Trp 62.

Because of the factors such as non-specific interactions, the normalized fluorescence change shown in figure 4(a) is not an ideal simple 1:1 binding. However, the 1:1 binding model is still a good approximation to give useful binding information. The linear correlation coefficient of the fitted line in figure 4(b) is 0.99, with $p < 0.001$. Also the fitted association constant is $(1.3 \pm 0.4) \times 10^5 \text{ M}^{-1}$ (average of four experiments).

3.5. Autodock computation results

The 30 binding models from the rough (with a large grid space of 0.503 Å) 'blind docking' calculation can be clustered into a

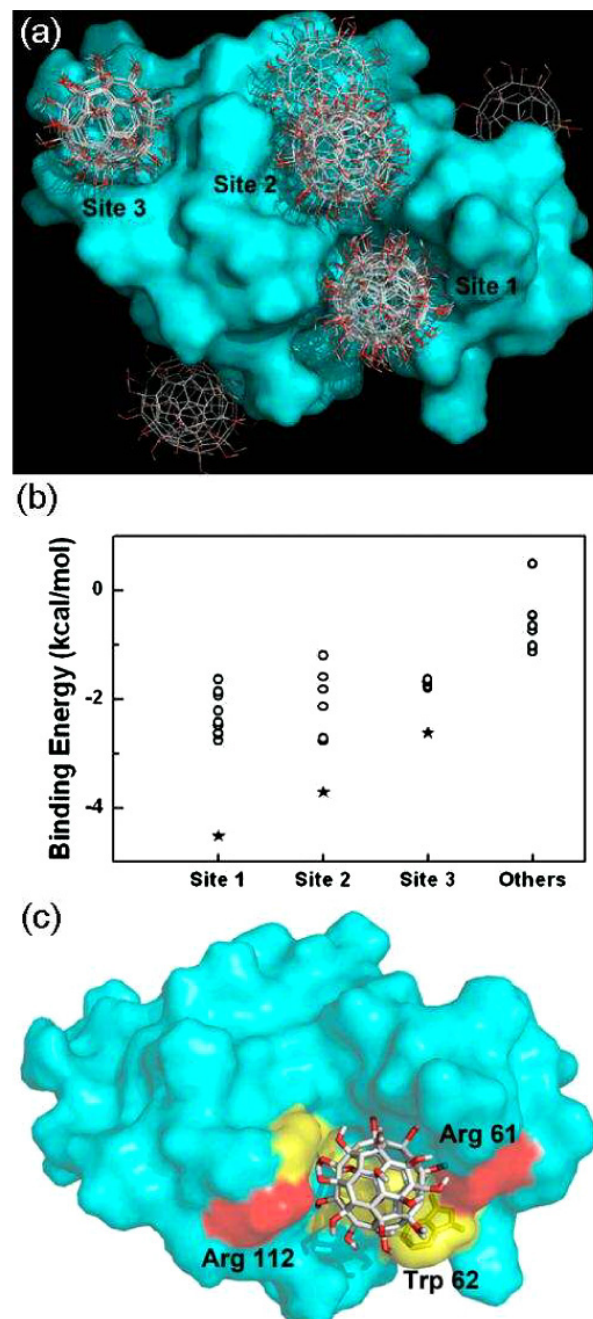


Figure 5. Autodock results of fullereneol-lysozyme complex. (a) Possible binding sites for fullereneol on lysozyme surface: site 1 contains 9 docking models, site 2 contains 7 models, site 3 contains 7 models, other sites (including one not visible on the rear surface of lysozyme) contain no more than 3 models. (b) Binding energy of the 30 'blind docking' models (open circles). The lowest energy models in the second round docking for sites 1, 2 and 3 were shown as asterisks. (c) The best binding model of the lysozyme-fullereneol complex computed using flexible docking. (a) and (c) were drawn using PyMOL (www.pymol.org).

(This figure is in colour only in the electronic version)

few binding sites, as shown in figure 5(a) (one invisible model located on the rear surface of lysozyme). All the top 13 lowest energy (figure 5(b)) models belong to site 1 (in total 9 models overlapped at site 1, 8 of them in the top 13) or site 2 (in

total 7 models overlapped at site 2, 5 of them in the top 13), making site 1 and site 2 the most likely binding places on lysozyme for fullerene. Site 3 contains 7 models, which is also a possible candidate. Other sites have only 1 to 3 models with much higher energy than the above three sites, showing less possibility as a binding site for fullerene. So, the second round dockings with smaller grid space (0.253 Å) were carried out to evaluate sites 1, 2 and 3 more accurately, with one grid box covering both site 1 and site 2, and a separate docking run with a different grid box covering site 3 only. The lowest binding energy from the second round docking calculating for site 1, site 2 and site 3 is $-4.5 \text{ kcal mol}^{-1}$, $-3.7 \text{ kcal mol}^{-1}$ and $-2.6 \text{ kcal mol}^{-1}$, respectively (indicated as asterisks in figure 5(b)), corresponding to the association constants of $2.0 \times 10^3 \text{ M}^{-1}$, $5.3 \times 10^2 \text{ M}^{-1}$ and $8.3 \times 10 \text{ M}^{-1}$, respectively. These data show that site 1 is the strongest binding site; site 2 and site 3, with almost 1 to 2 order of magnitudes weaker binding constant, only contribute significantly at very high concentration.

These computation results are very consistent with the aforementioned experimental results, even though no experimental information has been included in the computation. Binding site 1 locates in the end of the active cleft of lysozyme. Hence, binding of fullerene at this place certainly inhibits the activity of lysozyme, as shown in activity experiments. In addition, at binding site 1 the bound fullerene is close to Trp 62 (as well as Trp 63), thus changing the environment of Trp 62 (and Trp 63), resulting in the change of the near-UV CD spectra and fluorescence spectra, as shown in figures 3 and 4, respectively.

Both experimental evidence and computational results show that fullerene interacts with Trp 62 of lysozyme. In order to build an accurate binding model and evaluate the precise binding constant of fullerene with lysozyme, a flexible docking was performed with a grid box (0.203 Å grid spacing) covering site 1 using Autodock 4.0, with Trp 62 set as flexible residue. The binding model is shown in figure 5(c). The positive arginine (Arg) 112 and Arg 61 (in red in the electronic version) and aromatic residues around fullerene (in yellow in the electronic version) are shown, with Trp 62 shown as sticks. The calculated binding energy and association constant are $-6.96 \text{ kcal mol}^{-1}$ and $1.26 \times 10^5 \text{ M}^{-1}$, respectively. The experimentally determined association constant is $(1.3 \pm 0.4) \times 10^5 \text{ M}^{-1}$, corresponding to a binding energy of $-6.98 \text{ kcal mol}^{-1}$. At the current stage, the calculated binding energy is still of no significant meaning to correlate with the experimental one, even though our calculated and experimental binding energies match very well. But the calculated binding model does provide valuable information.

It is worth noting that Trp 62 is parallel to the near fullerene surface in the predicted model, which may form π - π stacking interaction. Interestingly, the binding site on a monoclonal fullerene-specific antibody for fullerene also contains VH Trp 47, as well as VL Tyr 91 and VL Phe 96, lying parallel to the C₆₀ molecule [45]. Experimental evidence shows that the binding site on human serum albumin (HSA) for fullerene contains the Trp 214 residue, and the docking model obtained using the PatchDock algorithm agreed with the experimental results [14]. Based on all those results,

we infer that a π - π stack interaction would be a common feature for the interaction of fullerenes, carbon nanotubes and their derivatives with proteins, and the proteins with partially exposed aromatic residues would more likely interact with fullerene and their derivatives. In fact, the π - π stacking interaction has already been widely used to noncovalently functionalize the carbon nanotubes [46].

4. Conclusion

In this study, we reveal that fullerene can specifically bind to hen egg white lysozyme, with an association constant of $(1.3 \pm 0.4) \times 10^5 \text{ M}^{-1}$. Fullerene slightly increases the thermal stability of lysozyme, but significantly inhibits the activity of lysozyme. Both the experimental and computational results suggest that the binding site on lysozyme for fullerene is close to Trp 62, and a π - π stacking interaction might play an important role in binding. We infer that π - π stacking may be a general mode for the interaction of fullerene and their derivatives with proteins, but how much the interaction will influence the activity of other proteins needs further individual analysis. To avoid the possible toxicity involved, a low dose of fullerene and derivatives used in the biomedical applications is preferable.

Acknowledgments

We thank the financial support from the China Natural Science Foundation (Significant Project nos. 10490180 and 20673003) and the China Ministry of Science and Technology (973 Project no. 2006CB705604).

References

- [1] Satoh M and Takayanagi I 2006 *J. Pharmacol. Sci.* **100** 513
- [2] Simic-Krstic J 1997 *Arch. Oncol.* **5** 143
- [3] Chen C Y *et al* 2005 *Nano Lett.* **5** 2050
- [4] Milic V D, Djordjevic A, Dobric S, Injac R, Vuckovic D, Stankov K, Simic V D and Suvajdzic Lj 2006 *Mater. Sci. Forum* **518** 525
- [5] Trajkovic S, Dobric S, Jacevic V, Dragojevic-Simic V, Milovanovic Z and Dordevic A 2007 *Colloids Surf. B* **58** 39
- [6] Meng X M, Chen Z, Li B, Zhang Y F, Zhao D X and Yang X L 2006 *Chin. Sci. Bull.* **51** 2550
- [7] Ryan J J, Bateman H R, Stover A, Gomez G, Norton S K, Zhao W, Schwartz L B, Lenk R and Kepley C L 2007 *J. Immunol.* **179** 665
- [8] Kane R S and Stroock A D 2007 *Biotechnol. Prog.* **23** 316
- [9] Rozhkov S P, Goryunov A S, Sukhanova G A, Borisova A G, Rozhkova N N and Andrievskiy G V 2003 *Biochem. Biophys. Res. Commun.* **303** 562
- [10] Prabha C R, Patel R and Murthy C N 2004 *Fullerenes Nanotub. Carbon Nanostruct.* **12** 405
- [11] Belgorodsky B, Fadeev L, Kolsenik J and Gozin M 2006 *ChemBioChem* **7** 1783
- [12] Deguchi S, Yamazaki T, Mukai S, Usami R and Horikoshi K 2007 *Chem. Res. Toxicol.* **20** 854
- [13] Belgorodsky B, Fadeev L, Ittah V, Benyamini H, Zelner S, Huppert D, Kotlyar A B and Gozin M 2005 *Bioconjug. Chem.* **16** 1058
- [14] Benyamini H, Shulman-Peleg A, Wolfson H J, Belgorodsky B, Fadeev L and Gozin M 2006 *Bioconjug. Chem.* **17** 378
- [15] Zhang X F, Shu C Y, Xie L, Wang C R, Zhang Y Z, Xiang J F, Li L and Tang Y L 2007 *J. Phys. Chem. C* **111** 14327

- [16] Baron M H, Revault M, Servagent-Noienville S, Abadie J and Quiquampoix H 1999 *J. Colloids Interface Sci.* **214** 319
- [17] Masschalck B and Michiels C W 2003 *Crit. Rev. Microbiol.* **29** 191
- [18] Sava G, Benetti A, Ceschia V and Pacor S 1989 *Anticancer Res.* **9** 583
- [19] Rymuszka A, Studnicka M, Siwicki A K, Sleroslawska A and Bownik A 2005 *Ecotoxicol. Environ. Safety* **61** 121
- [20] Blake C C F, Koenig D F, Mair G A, North A C T, Phillips D C and Sarma V R 1965 *Nature* **206** 757
- [21] Radford S E, Dobson C M and Evans P A 1992 *Nature* **358** 302
- [22] Cao A N, Wang G, Lai L H and Tang Y Q 2002 *Biochem. Biophys. Res. Commun.* **291** 795
- [23] Cao A N, Hu D Y and Lai L H 2004 *Protein Sci.* **13** 319
- [24] Lai B, Cao A N and Lai L H 2000 *Biochim. Biophys. Acta* **1543** 115
- [25] Lu R C, Cao A N, Lai L H and Xiao J X 2007 *Colloid Surf. B* **54** 20
- [26] Luckarift H R, Dickerson M B, Sandhage K H and Spain J C 2006 *Small* **2** 640
- [27] Li J, Takeuchi A, Ozawa M, Li X H, Saigo K and Kitazawa K 1993 *J. Chem. Soc., Chem. Commun.* **23** 1784
- [28] Ji Z Q, Sun H F, Wang H F, Xie Q Y, Liu Y F and Wang Z 2006 *J. Nanopart. Res.* **8** 53
- [29] Shugar D 1952 *Biochim. Biophys. Acta* **8** 302
- [30] Sheehan D 2000 *Physical Biochemistry: Principles and Applications* (New York: Wiley) p 83
- [31] Lee V S, Nimmanpipug P, Aruksakunwong O, Promsri S, Sompornpisut P and Hannongbua S 2007 *J. Mol. Graph. Model* **26** 558
- [32] Akaho E, Morris G, Goodsell D, Wong D and Olson A 2001 *J. Chem. Software* **7** 103
- [33] Sanner M F 1999 *J. Mol. Graph. Model* **17** 57
- [34] Vilenó B, Marcoux P R, Lekka M, Sienkiewicz A, Fehér T and Forró L 2006 *Adv. Funct. Mater.* **16** 120
- [35] Friedman S H, DeCamp D L, Sijbesma P R, Srdanov G, Wudl F and Kenyon G L 1993 *J. Am. Chem. Soc.* **115** 6506
- [36] Sijbesma R, Srdanov G, Wudl F, Castoro J A, Wilkins C, Friedman S H, DeCamp D L and Kenyon G L 1993 *J. Am. Chem. Soc.* **115** 6510
- [37] Chen B X, Wilson S R, Das M, Coughlin D J and Erlanger B F 1998 *Proc. Natl Acad. Sci. USA* **95** 10809
- [38] Lu L H, Lee Y T, Chen H W, Chiang L Y and Huang H C 1998 *Br. J. Pharmacol.* **123** 1097
- [39] Xia T, Kovoichich M, Brant J, Hotze M, Sempf J, Oberley T, Sioutas C, Yeh J I, Wiesner M R and Nel A E 2006 *Nano Lett.* **6** 1794
- [40] Isakovic A *et al* 2006 *Toxicol. Sci.* **91** 173
- [41] Sayes C M, Marchione A A, Reed K L and Warheit D B 2007 *Nano Lett.* **7** 2399
- [42] Usenko C Y, Harper S L and Tanguay R L 2007 *Carbon* **45** 1891
- [43] Privalov P L and Makhatadze G I 1992 *J. Mol. Biol.* **224** 715
- [44] Greenfield N and Fasman G D 1969 *Biochemistry* **8** 4108
- [45] Braden B C, Goldbaum F A, Chen B X, Kirschner A N, Wilson S R and Erlanger B F 2000 *Proc. Natl Acad. Sci. USA* **97** 12193
- [46] Chen R J, Zhang Y G, Wang D W and Dai H J 2001 *J. Am. Chem. Soc.* **123** 3838